

## 在 LiCl-KCl 共晶熔体中电化学制备钬镍金属间化合物

李 梅 孙婷婷 韩 伟\* 王珊珊 张密林 颜永得 张 萌

(哈尔滨工程大学材料科学与化学工程学院, 教育部超轻材料与表面技术重点实验室, 哈尔滨 150001)

**摘要:** 采用循环伏安、方波伏安和开路计时电位等方法研究了 Ho(III) 离子在 LiCl-KCl 共晶熔体中的电化学行为及 Ho-Ni 合金化机理。在惰性 W 电极上, Ho(III) 离子在 -2.06 V(vs Ag/AgCl) 发生电化学还原, 该还原过程为 3 个电子转移的一步反应。与惰性 W 电极上的循环伏安相比, Ho(III) 离子在活性 Ni 电极的循环伏安曲线上还出现了 3 对氧化还原峰, 是 Ho 与 Ni 形成了金属间化合物, 导致了 Ho(III) 离子在活性 Ni 电极发生了欠电位沉积。在不同的电位进行恒电位电解制备的 3 个不同的 Ho-Ni 合金, 采用 X-射线衍射(XRD)和扫描电子显微镜-能谱仪(SEM-EDS)等测试手段进行表征, 结果表明: 制备的 3 种合金分别是 Ho<sub>2</sub>Ni<sub>17</sub>, HoNi<sub>5</sub> 和 HoNi<sub>2</sub> 3 种合金化合物。

**关键词:** 电化学行为; 钬-镍合金化合物; 恒电位电解; 镍电极

中图分类号: 0614.111; 0614.22; TB323

文献标识码: A

文章编号: 1001-4861(2015)01-0177-06

DOI: 10.11862/CJIC.2015.006

## Electrochemical Preparation of Ho-Ni Intermetallic Compounds in LiCl-KCl Eutectic Melts

LI Mei SUN Ting-Ting HAN Wei\* WANG Shan-Shan ZHANG Mi-Lin YAN Yong-De ZHANG Meng

(Key Laboratory of Superlight Materials and Surface Technology, Ministry of Education, College of Material Science and Chemical Engineering, Harbin Engineering University, Harbin 150001, China)

**Abstract:** The electrochemical behavior of Ho(III) in LiCl-KCl eutectic melts and the alloying mechanism of Ho-Ni alloys were investigated by cyclic voltammetry, square wave voltammetry and open circuit chronopotentiometry. On an inert W electrode, the electroreduction of Ho(III) proceeds in a one-step process involving three electrons at -2.06 V (vs Ag/AgCl). Compared with the cyclic voltammograms on an inert W electrode, three reduction peaks are observed which indicates the under-potential deposition of Ho(III) on the reactive Ni electrode due to the formation of Ho-Ni intermetallic compounds. Three alloy samples were produced by potentiostatic electrolysis at various potentials and characterized by X-ray diffraction (XRD), scanning electron microscopy and energy dispersive spectrometer (SEM-EDS), respectively. The results confirm the three alloy samples of Ho<sub>2</sub>Ni<sub>17</sub>, HoNi<sub>5</sub> and HoNi<sub>2</sub> intermetallic compounds, respectively.

**Key word:** electrochemical behavior; Ho-Ni intermetallic compounds; potentiostatic electrolysis; LiCl-KCl melts

As structural and functional materials, intermetallic compounds have attracted considerable attention due to their high potential for various applications<sup>[1-3]</sup>. The rare earth-Ni intermetallic compounds are essential for high-temperature structural

materials, magnetic materials, catalytic, hydrogen storage alloys, etc<sup>[4-5]</sup>. As a new preparation method of the rare earth-transition metal intermetallic compounds, electrochemical synthesis using molten salts is an effective method because composition and thickness of

收稿日期: 2014-06-30。收修稿日期: 2014-10-08。

国家自然科学基金(No.21271054, 21173060, 51104050), 国家自然科学基金重大项目(No.91326113, 91226201)以及中央高校研究基金(HEUCF201403001)资助项目。

\*通讯联系人。E-mail: weihan@hrbeu.edu.cn, Tel: 0451-82569890; 会员登记号: S06N3035M1005。

the alloys can be controlled by electrochemical parameters<sup>[6]</sup>. Kobayashi et al.<sup>[7-8]</sup> and Yasuda et al.<sup>[9-10]</sup> have investigated the electrochemical formation of Dy-Ni and Nd-Ni alloys in a molten LiF-CaF<sub>2</sub>-LnF<sub>3</sub> and NaCl-KCl-LnCl<sub>3</sub> (Ln=Dy and Nd) melts, respectively. Chamelot and co-worker<sup>[11]</sup> have obtained NdNi<sub>2</sub>, NdNi<sub>3</sub>, GdNi<sub>2</sub>, GdNi, Ni<sub>2</sub>Sm and Ni<sub>3</sub>Sm intermetallic compounds on a reactive nickel electrode by the electroreduction of the lanthanides (Nd, Gd and Sm) in LiF-CaF<sub>2</sub>-LnF<sub>3</sub> molten salts. Nohira et al.<sup>[12]</sup> have studied the electrochemical preparation of Pr-Ni alloys in a molten LiCl-KCl-PrCl<sub>3</sub> (0.50 mol %) system. Iida and co-worker<sup>[13-14]</sup> have explored the formation of Sm-Ni and Yb-Ni alloys in a molten LiCl-KCl-LnCl<sub>3</sub> (Ln=Sm and Yb) melts. Yang and co-worker<sup>[15]</sup> have explored the electroreduction of Ho<sup>3+</sup> on nickel cathode in molten KCl-HoCl<sub>3</sub>. The free energies of formation for the intermetallic compounds between Ho and Ni, the diffusion coefficients and diffusion activation energy of Ho atom in the alloy phase were determined.

Since the operation conditions significantly influences the feasibility of pyrometallurgical reprocessing, it is of crucial importance to have the knowledge of the electrochemical behavior of Ln in different melts for the understanding of the process. The electrochemical reduction of Ho(III) on a Ni electrode has only been studied in the KCl system<sup>[15]</sup>, whereas the LiCl-KCl eutectic melts has not been used for the electrochemical synthesis of Ho-Ni alloys. Thus, the electrochemical behavior of Ho(III) was studied on an inert W electrode and a reactive Ni electrode in LiCl-KCl-HoCl<sub>3</sub> melts by cyclic voltammetry, square wave voltammetry and open circuit chronopotentiometry. The preparation of Ho-Ni intermetallic compounds was carried out by potentiostatic electrolysis at different potentials, and the samples were characterized by XRD and SEM-EDS.

## 1 Experimental

### 1.1 Preparation and purification of the melt

A mixture of LiCl-KCl eutectic melts (58.5:41.5, *n/n*) (analytical grade) was first dried under vacuum for more than 48 h at 573 K to remove excess water and

then melted in an alumina crucible located in an electric furnace. The temperature of the melts was measured with a nickel chromium-nickel aluminium thermocouple sheathed with an alumina tube. Metal ion impurities in the melts were removed by pre-electrolysis at -2.10 V (vs Ag/AgCl) for 4 h. Anhydrous HoCl<sub>3</sub> (99.9wt%; High Purity Chemical Co. Ltd.) was added directly to the melts as a Ho(III) ion source.

### 1.2 Electrochemical apparatus and electrodes

All electrochemical measurements were performed using an Autolab PGSTAT 302N (Metrohm, Ltd.) with NOVA 1.8 software where techniques of cyclic voltammetry (CV), square wave voltammetry (SWV) and open circuit chronopotentiometry (OCP) were employed. The working electrodes were W wire (*d*=1 mm; 99.99%) and Ni plate (2 mm×11 mm; 99.99%), which were polished thoroughly using SiC paper (2000 grit), and then cleaned ultrasonically with dilute hydrochloric acid and ethanol prior to use. The Ag/AgCl electrode (Ag; *d*=1 mm; 99.99%) used as reference electrode (RE) was encased in a Pyrex tube, in which the LiCl-KCl eutectic melts contain 1.0wt% AgCl (99.998%). All potentials are referred to the Ag/AgCl couple.

### 1.3 Characterization of deposits

The deposits were prepared by potentiostatic electrolysis under different conditions. After electrolysis, the alloy samples were washed in hexane (99.8 %) in an ultrasonic bath to remove salts and stored in a glove box for analysis. These deposits were analyzed by X-ray diffraction (XRD, X' Pert Pro; Philips Co., Ltd.) using Cu K $\alpha$  radiation ( $\lambda$ =0.154 06 nm) at 40 kV and 150 mA with a  $2\theta$ - $\theta$  scan mode in the  $2\theta$  range of 20°~90°, and the step size was 0.02°. The microstructure and micro-zone chemical analysis were measured by scanning electron microscopy and energy dispersive spectrometer (SEM-EDS, JSM-6480A, JEOL Co., Ltd.) under conditions of accelerating voltage of 20.0 kV, the valid time of 30.0 s and the incident angle of 90.0°.

## 2 Results and discussion

### 2.1 Electrochemical behavior of Ho(III) ions in LiCl-KCl eutectic melts on a W electrode

#### 2.1.1 Cyclic Voltammetry

Fig.1 presents the typical cyclic voltammograms (CVs) obtained in the LiCl-KCl melts before and after the addition of  $\text{HoCl}_3$  at 1 023 K. On the dotted curve, peaks A and A' correspond to the deposition and dissolution of Li metal, since no alloys or intermetallic compounds exist in the W-Li phase diagram<sup>[16]</sup> at 1 023 K. The solid curve represents the CVs after the addition of  $\text{HoCl}_3$  in the LiCl-KCl melts. Except for the cathodic/anodic peaks A/A', the peaks B/B' observed at  $-2.06 \sim -1.89$  V (vs Ag/AgCl) are ascribed to the deposition and subsequent reoxidation of holmium.

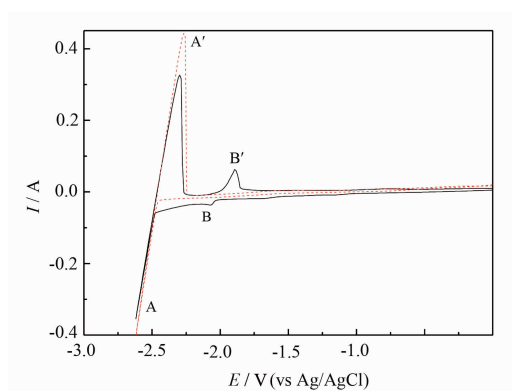


Fig.1 Typical CVs of the LiCl-KCl melts before (dotted line) and after (solid line) the addition of  $\text{HoCl}_3$  ( $2.50 \times 10^{-4} \text{ mol} \cdot \text{cm}^{-3}$ ) on a W electrode ( $S=0.322 \text{ cm}^2$ ) at 1 023 K. Scan rate:  $0.1 \text{ V} \cdot \text{s}^{-1}$

### 2.1.2 Square wave voltammetry

The square wave voltammetry technique was used to determine the number of electrons involved in the electrochemical step. For a simple reversible reaction, the width of the half-peak,  $W_{1/2}$ , depends on the number of electrons exchanged and on the temperature as follows<sup>[17]</sup>:

$$W_{1/2} = 3.52RT/(nF) \quad (1)$$

where  $R$  is the universal gas constant,  $T$  is the absolute temperature (K),  $n$  is the number of exchanged electrons, and  $F$  is the Faradays constant ( $96\,485 \text{ C} \cdot \text{mol}^{-1}$ ).

Fig.2 shows a square wave voltammogram obtained in the LiCl-KCl- $\text{HoCl}_3$  melts on a W electrode. The peak shown in Fig.2 exhibits an asymmetrical Gaussian signal attributed to the nucleation overpotential, the rise of the current is delayed by the overpotential caused by the solid phase formation. The relationship (1) can be

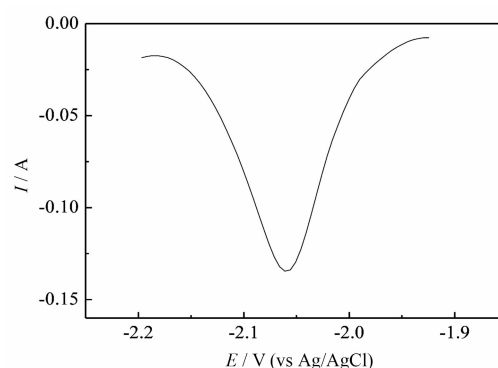


Fig.2 Square wave voltammogram of the LiCl-KCl- $\text{HoCl}_3$  ( $2.50 \times 10^{-4} \text{ mol} \cdot \text{cm}^{-3}$ ) melts obtained on a W electrode ( $S=0.322 \text{ cm}^2$ ) at 1 023 K. Pulse height: 25 mV; potential step: 1 mV; frequency, 30 Hz

utilized to calculate the number of electrons involved in the reduction reactions of  $\text{Ho(III)}/\text{Ho(0)}$  when we apply this technique at low frequencies and small step potentials<sup>[17-18]</sup>. Using this methodology, the value of  $n$  is 2.86, close to three electrons, which indicates that the electroreduction of  $\text{Ho(III)}$  proceeds in a one-step process involving three electrons. The result is consistent with the ones obtained from the cyclic voltammograms.

## 2.2 Electrochemical behavior of $\text{Ho(III)}$ ions on a nickel electrode and formation of Ho-Ni intermetallic compounds

### 2.2.1 Electrochemical behavior of $\text{Ho(III)}$ ions in LiCl-KCl eutectic melts on a Ni electrode

In order to investigate the formation of Ho-Ni intermetallic compounds, cyclic voltammetry was conducted on a Ni electrode in the LiCl-KCl- $\text{HoCl}_3$  melts. Fig.3 shows the typical CVs of the LiCl-KCl melts before (dotted line) and after (solid line) the addition of  $\text{HoCl}_3$  ( $2.50 \times 10^{-4} \text{ mol} \cdot \text{cm}^{-3}$ ) on a Ni electrode at 1 023 K. On the dotted curve in Fig.3, comparison to the CVs of the LiCl-KCl melts on a W electrode, the peaks A/A' correspond to the deposition and re-oxidation of Li metal. The sharp increase signals F/F' can be ascribed to the deposition and dissolution of Ni metal.

The shape of the solid curve in Fig.3 obtained on a Ni electrode is very different from the one obtained on a W electrode after the addition of  $\text{HoCl}_3$  in the LiCl-KCl melts (solid curve in Fig.1). Except for the peaks A/A'

and B/B' at  $-2.42$  V/ $-2.33$  V and  $-2.06$  V/ $-1.89$  V (vs Ag/AgCl), corresponding to the reduction/oxidation of lithium and holmium, respectively, additional peaks appear prior to the reduction of Ho(III) to give pure metal on a W electrode. Of evidence, these peaks, C/C', D/D' and E', are attributed to the formation and re-oxidation of Ho-Ni intermetallic compounds.

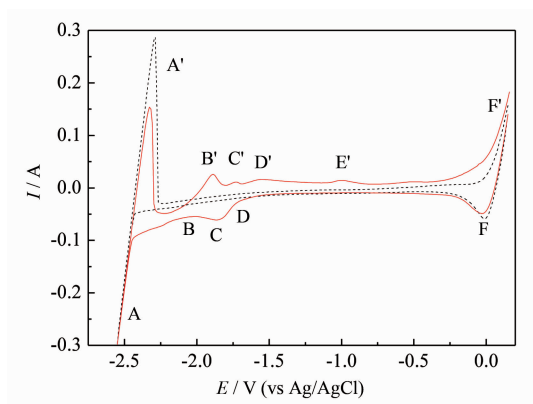


Fig.3 Typical CVs of the LiCl-KCl melts before (dotted line) and after (solid line) the addition of  $\text{HoCl}_3$  on a Ni electrode ( $S=0.322\text{ cm}^2$ ) at  $1\,023\text{ K}$ . Scan rate:  $0.1\text{ V}\cdot\text{s}^{-1}$

In addition, square wave voltammetry was employed to further investigation of the electrochemical behavior of Ho(III) on a Ni electrode, since square wave voltammetry is more sensitive and has a higher resolution than cyclic voltammetry<sup>[19]</sup>. Fig.4 shows a square wave voltammogram obtained at a step potential of  $1\text{ mV}$  and frequency of  $30\text{ Hz}$  in the LiCl-KCl- $\text{HoCl}_3$  ( $2.50\times 10^{-4}\text{ mol}\cdot\text{cm}^{-3}$ ) melts on a Ni electrode at  $1\,023\text{ K}$ . It exhibits four peaks B, C, D, and E, corresponding

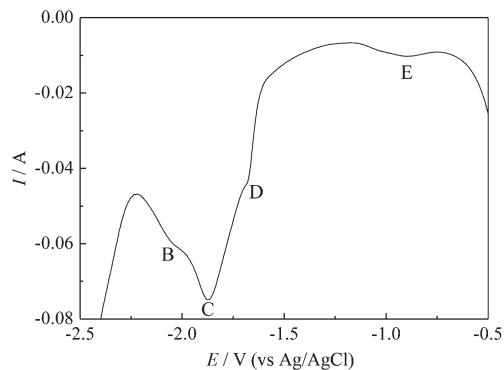


Fig.4 Square wave voltammogram of the LiCl-KCl- $\text{HoCl}_3$  melts obtained on a Ni electrode ( $S=0.322\text{ cm}^2$ ) at  $1\,023\text{ K}$ ; Pulse height:  $25\text{ mV}$ ; potential step:  $1\text{ mV}$ ; frequency:  $30\text{ Hz}$

to the reactions of Ho(III)/Ho(0), the formation of three different intermetallic compounds, respectively, which is consistent with the results obtained from cyclic voltammogram on a Ni electrode.

Open circuit chronopotentiometry was carried out to further investigate the formation of Ho-Ni intermetallic compounds. Since the deposited Ho metal reacts with Ni and diffuses into the Ni electrode, the electrode potential gradually shifts to more positive values. During this process, a potential plateau is observed when the composition of the electrode surface is within a range of a two-phase coexisting state<sup>[13,20]</sup>. Fig. 5 shows an open circuit chronopotentiogram after potentiostatic electrolysis at  $-2.60\text{ V}$  (vs Ag/AgCl) for  $35\text{ s}$  on a Ni electrode. Five potential plateaus are observed at  $-2.28$ ,  $-2.01$ ,  $-1.82$ ,  $-1.61$  and  $-1.10\text{ V}$  (vs Ag/AgCl), respectively. The first potential plateau A is thought to be due to the presence of the codeposited Li metal on the electrode. The second plateau B is considered to be ascribed to the Ho(III)/Ho(0) potential. After that, three plateaus C, D and E correspond to the coexisting states of different Ho-Ni intermetallic compounds.

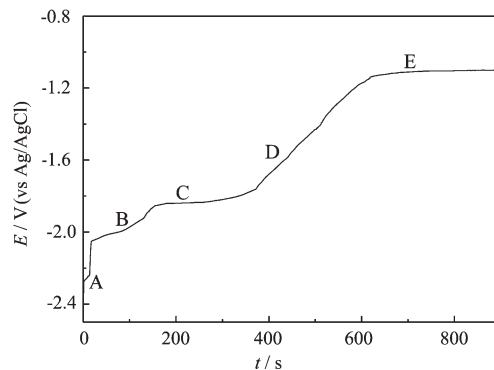


Fig.5 Open circuit potentiogram of LiCl-KCl- $\text{HoCl}_3$  ( $2.50\times 10^{-4}\text{ mol}\cdot\text{cm}^{-3}$ ) melts on a Ni electrode ( $S=0.322\text{ cm}^2$ ) at  $-2.6\text{ V}$  vs Ag/AgCl for  $35\text{ s}$  at  $1\,023\text{ K}$

## 2.2.2 Potentiostatic electrolysis and characterization of deposits

Based on the results of cyclic voltammogram, square wave voltammogram and open circuit potentiogram, the Ho-Ni alloy compounds were prepared by potentiostatic electrolysis on a Ni electrode

( $S=2.88 \text{ cm}^2$ ) in the LiCl-KCl-HoCl<sub>3</sub> ( $2.50 \times 10^{-4} \text{ mol cm}^{-3}$ ) melts.

Fig.6 shows the XRD patterns of Ho-Ni alloy samples obtained by potentiostatic electrolysis in the

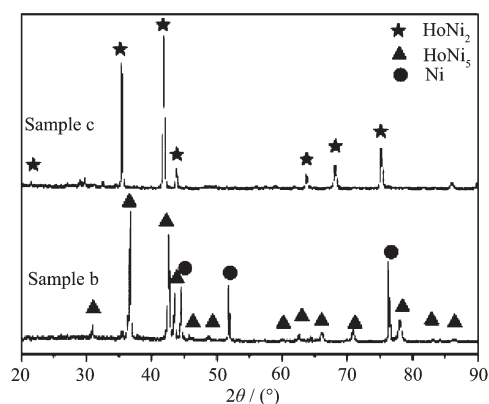


Fig.6 XRD patterns of the deposits obtained by potentiostatic electrolysis in the LiCl-KCl-HoCl<sub>3</sub> melts on a Ni electrode at 1 023 K; sample b: at  $-1.8 \text{ V}$  for 10 h; sample c at  $-2.2 \text{ V}$  for 10 h

LiCl-KCl-HoCl<sub>3</sub> melts at  $-1.8 \text{ V}$  (1 023 K, 10 h, sample (b)) and  $-2.2 \text{ V}$  (1 023 K, 10 h, sample (c)), respectively. XRD patterns indicate that the Ho-Ni alloy samples are comprised of HoNi<sub>5</sub> and HoNi<sub>2</sub>, respectively.

At  $-1.8 \text{ V}$  (vs Ag/AgCl), the sample (a) was obtained by potentiostatic electrolysis at  $-1.8 \text{ V}$  for 5 h. The cross-sectional SEM image of the sample (a) in Fig. 7a shows the thickness of the alloy layer is around  $20 \mu\text{m}$ . The EDS point analysis of labeled A in the Fig. 7a shows that the atomic ratio of Ni to Ho is about 17:2 (Fig.7b). Because the alloy layer is very thin, there is no corresponding signal can be detected by XRD. Nohira et al.<sup>[6]</sup> pointed out that one phase forms preferentially and another phase starts to form upon the completion of the preferentially phase formation. According to the Ho-Ni phase diagram<sup>[21]</sup> and the analysis of EDS, we think the observed alloy layer in the sample (a) is Ho<sub>2</sub>Ni<sub>17</sub> layer with  $20 \mu\text{m}$  thickness.

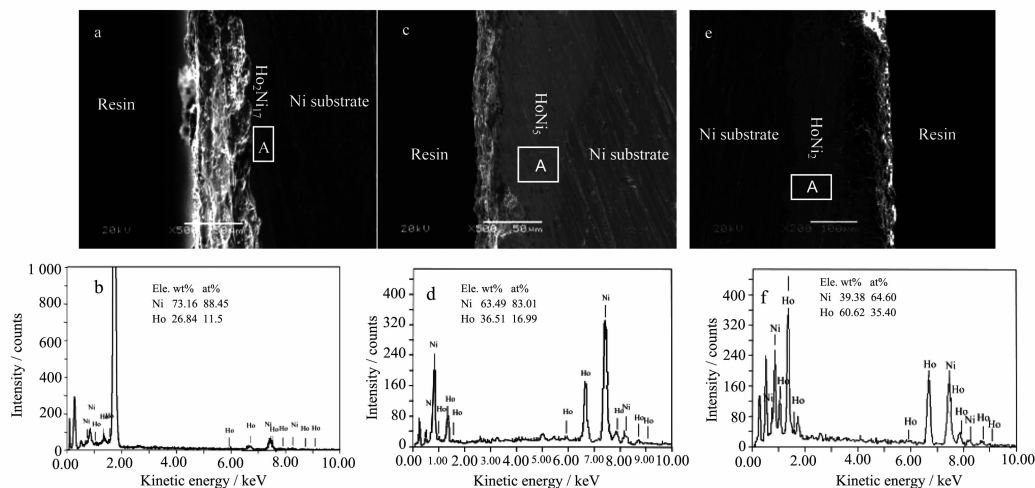


Fig.7 SEM and EDS analysis of the Ho-Ni alloys obtained by potentiostatic electrolysis in the LiCl-KCl-HoCl<sub>3</sub> melts; SEM image (a) and EDS point analysis (b) at  $-1.8 \text{ V}$  for 5 h; SEM image (c) and EDS point analysis (d) at  $-1.8 \text{ V}$  for 10 h; SEM image (e) and EDS point analysis (f) at  $-2.2 \text{ V}$  for 10 h

Fig.7c shows the SEM image of sample (b) obtained at  $-1.8 \text{ V}$  (vs Ag/AgCl) for 10 h at 1 023 K. The thickness of alloy layer is close to  $60 \mu\text{m}$ . The EDS of labeled A in Fig.7c indicates that the atomic ratio of Ni to Ho is close to 5:1 (Fig.7d). The XRD pattern confirms the presence of HoNi<sub>5</sub> in the sample (b). At the same potential, the Ho-Ni intermetallic compound obtained is different at different electrolysis time. The longer the

electrolysis time, the richer Ho intermetallic compound is obtained by potentiostatic electrolysis at the same potential.

At  $-2.2 \text{ V}$ , only one intermetallic compound HoNi<sub>2</sub> is characterized by XRD in Fig.6. The cross-sectional SEM image of the sample (c) is presented in Fig.7e. The result shows that the thickness of deposited alloy layer is about  $130 \mu\text{m}$  and the atomic ratio of Ni to Ho is

close to 2:1 (Fig.7f). Combined with the XRD pattern of the sample (c) in Fig.6, we think that the alloy layer is a uniform HoNi<sub>2</sub> layer.

### 3 Conclusions

The electrochemical behavior of Ho(III) in the eutectic LiCl-KCl melts on W and Ni electrodes were investigated by a series of electrochemical techniques. The results show that the reduction mechanism of Ho(III) proceeds in a one-step process exchanging three electrons on a W electrode. The under-potential deposition of Ho(III) on a Ni electrode is due to the formation of different Ho-Ni intermetallic compounds. According to the study of cyclic voltammograms, square wave voltammogram and open-circuit chronopotentiograms, the Ho-Ni intermetallic compounds were obtained by potentiostatic electrolysis under different potentials. The formation of Ho-Ni alloys with different ratios of the two metals, i.e. Ho<sub>2</sub>Ni<sub>17</sub>, HoNi<sub>5</sub> and HoNi<sub>2</sub>, is confirmed by XRD, SEM-EDS.

### References:

- [1] Yaropolov Y L, Andreenko A S, Nikitin S A, et al. *J. Alloys Compd.*, **2011**,**509**:S830-834
- [2] Haraguchi T, Kogachi M. *Mater. Sci. Eng. A*, **2002**,**329-331**: 402-407
- [3] GUO Xin(郭欣), LI Shu-Cun(李书存), WANG Li(王丽) et al. *Chinese J. Inorg. Chem.*(无机化学学报), **2014**,**30**(9):2019-2024
- [4] Domnguez-Crespo M A, Torres-Huerta A M, Brachetti-Sibaja B, et al. *Int. J. Hydrogen Energy*, **2011**,**36**:135-151
- [5] Li P, Li Q Q, Jin T, et al. *Mater. Sci. Eng. A*, **2014**,**603**:84-92
- [6] Konishi H, Nohira T, Ito Y. *Electrochim. Acta*, **2003**,**48**:563-568
- [7] Kobayashi S, Nohira T, Kobayashi K, et al. *J. Electrochem. Soc.*, **2012**,**159**(12):E193-197
- [8] Kobayashi S, Kobayashi K, Nohira T, et al. *J. Electrochem. Soc.*, **2011**,**158**(12):E142-146
- [9] Yasuda K, Kobayashi S, Nohira T, et al. *Electrochim. Acta*, **2013**,**106**:293-300
- [10] Yasuda K, Kobayashi S, Nohira T, et al. *Electrochim. Acta*, **2013**,**92**:349-355
- [11] Chamelot P, Massot L, Hamel C, et al. *J. Nucl. Mater.*, **2007**,**360**:64-74
- [12] Nohira T, Kambara H, Amezawa K, et al. *J. Electrochem. Soc.*, **2005**,**152**(4):C183-189
- [13] Iida T, Nohira T, Ito Y, et al. *Electrochim. Acta*, **2001**,**46**: 2537-2544
- [14] Iida T, Nohira T, Ito Y, et al. *Electrochim. Acta*, **2003**,**48**: 1531-1536
- [15] SU Yu-Zhi(苏育志), YANG Qi-Qin(杨绮琴), LIU Guan-Kun(刘冠昆). *J. Rare Earths*, **2000**,**18**(1): 34-38
- [16] Sangster J, Pelton A D. *J. Phase Equilib.*, **1991**,**12**:203
- [17] Bard A J, Faulkner L R. *Electrochemical Methods: Fundamental and Applications*. New York: John Wiley & Sons, Inc, **2001**:291
- [18] Castrillejo Y, Fernández P, Bermejo M R, et al. *Electrochim. Acta*, **2009**,**54**:6212-6222
- [19] Strycker J D, Westbroek P, Temmerman E. *Electrochem. Commun.*, **2002**,**4**:41-46
- [20] Konishi H, Nishikiori T, Nohira T. *Electrochim. Acta*, **2003**,**48**:1403-1408
- [21] Zhou H Y, Ou X L, Zhong X P. *J. Alloys Compd.*, **1991**,**117** (1):102-106